INTERNATIONAL JOURNAL FOR NUMERICAL METHODS IN FLUIDS
Int. J. Numer. Meth. Fluids 2008; **56**:1441–1447
Published online 20 September 2007 in Wiley InterScience (www.interscience.wiley.com). DOI: 10.1002/fld.1599

A cell by cell anisotropic adaptive mesh ALE method

J. M. Morrell[1], P. K. Sweby[1,*,†] and A. Barlow[2]

[1] *Department of Mathematics, The University of Reading, P.O. Box 220, Reading RG6 6AX, U.K.*
[2] *AWE, Aldermaston, Reading RG7 4PR, U.K.*

SUMMARY

A cell by cell anisotropic adaptive mesh Arbitrary Lagrangian Eulerian (ALE) method for the solution of the Euler equations is described. An efficient approach to equipotential mesh relaxation on anisotropically refined meshes is developed. Results for two test problems are presented. © British Crown Copyright 2007/MOD. Reproduced with permission. Published by John Wiley & Sons, Ltd.

Received 27 April 2007; Revised 15 July 2007; Accepted 16 July 2007

KEY WORDS: ALE—Arbitrary Lagrangian Eulerian; adaptivity; mesh adaptation; finite element methods; hydrodynamics; compressible flow

1. INTRODUCTION

Increasing mesh resolution around features of interest, such as shocks, without requiring a prohibitively large number of elements and nodes may be achieved by moving the mesh nodes or locally increasing the number of elements (h-refinement).

Moving the nodes in a Lagrangian manner can concentrate nodes around the features of interest and align the mesh with the directions of flow. However, the mesh may become tangled and a mesh relaxation strategy may be required to reduce tangling and improve the quality of the mesh. The staggered mesh Arbitrary Lagrangian Eulerian (ALE) method consists of: solving the Lagrangian formulation of the Euler equations using finite elements for the spatial derivatives and a predictor–corrector time advancement scheme; relaxing the Lagrangian mesh using Winslow's equipotential mesh relaxation method [1–3]; remapping or advecting the solution onto the new relaxed mesh.

[*] Correspondence to: P. K. Sweby, Department of Mathematics, The University of Reading, P.O. Box 220, Reading RG6 6AX, U.K.
[†] E-mail: p.k.sweby@reading.ac.uk

Contract/grant sponsor: AWE, Aldermaston

In this paper we combine the existing ALE method [1] with additional adaptivity in the form of element subdivision (h-refinement), thereby focusing resolution locally around the features of interest without requiring global refinement of the entire mesh.

Many features of interest involve large changes in variable in one dominant direction only. Anisotropic refinement allows the resolution to be increased in the dominant direction without unnecessary extra elements in the other direction. Anisotropic refinement aligned with an element's local directions, ξ and η, can be particularly efficient and beneficial, since the ALE mesh is aligned with the features of interest and flow directions.

2. METHOD

The elements are subdivided anisotropically in their ξ or η direction, or isotropically in both directions. Whether refinement occurs and the type of refinement is indicated by the element's change in density $\Delta\rho = \Delta\rho_\xi \hat{\boldsymbol{\xi}} + \Delta\rho_\eta \hat{\boldsymbol{\eta}}$, where, for example,

$$|\Delta\rho_\xi| = \max[|\rho_r - \rho_i|, |\rho_i - \rho_l|] \tag{1}$$

and ρ_i is the coarse element's density, ρ_l is the coarse density in the left neighbour element and ρ_r is the coarse density in the right neighbour element.

If $|\Delta\rho|$ is greater than the refinement radius then the element is refined. The ratio of the components $|\Delta\rho_\eta|$ and $|\Delta\rho_\xi|$ is used to decide whether anisotropic or isotropic refinement is required [4]

$$\begin{aligned} \frac{|\Delta\rho_\eta|}{|\Delta\rho_\xi|} &< \tan(30°) \Rightarrow \xi\text{-refinement} \\ \tan(30°) < \frac{|\Delta\rho_\eta|}{|\Delta\rho_\xi|} &< \tan(60°) \Rightarrow \text{isotropic refinement} \\ \frac{|\Delta\rho_\eta|}{|\Delta\rho_\xi|} &> \tan(60°) \Rightarrow \eta\text{-refinement} \end{aligned} \tag{2}$$

Fine elements are derefined if $|\Delta\rho|$ drops below the derefinement threshold. Isotropic to anisotropic derefinement is triggered when the $\Delta\rho$ angle is below the derefinement angle (25°).

In this work cell by cell refinement is used rather than selecting a rectangular block or cluster of elements to be refined simultaneously as in structured AMR [5–7]. New elements are inserted into the mesh forming an unstructured combined mesh referred to as the Dynamic Mesh. The Dynamic Mesh consists of the highest resolution existing for each part of the domain, with disjoint or hanging nodes that have three nodal neighbours rather than four at resolution transitions.

The Euler equations are solved on the Dynamic Mesh rather than solving for every resolution level separately as is done in structured AMR [5–7]. Disjoint nodes are considered non-dynamic points; they do not have nodal mass or force associated with them and therefore these quantities are redistributed to the neighbouring dynamic nodes. The position and velocity of the disjoint node n_D are 'slaved', for example, $\mathbf{u}_{n_\text{D}} = \frac{1}{2}\mathbf{u}_{n_1} + \frac{1}{2}\mathbf{u}_{n_2}$, where n_1 and n_2 are the nodes either side of the disjoint node on that interface.

Winslow's equipotential mesh relaxation method [1–3] and the remapping procedure [1] are generalized so that they can be efficiently applied directly to the Dynamic Mesh, rather than

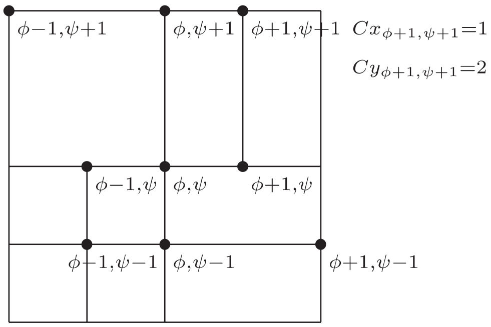

Figure 1. Stencil for a Dynamic Mesh node.

decomposing the Dynamic Mesh into refinement levels. Winslow's method calculates a node's new relaxed position using a 9-point nodal stencil and central differences to discretize the inverse Laplace equation

$$\frac{\alpha}{4}\frac{\partial^2 x}{\partial\phi^2}-\beta\frac{\partial^2 x}{\partial\phi\psi}+\frac{\gamma}{4}\frac{\partial^2 x}{\partial\psi^2}=0 \tag{3}$$

where

$$\alpha=4\left(\left(\frac{\partial x}{\partial\psi}\right)^2+\left(\frac{\partial y}{\partial\psi}\right)^2\right) \tag{4}$$

$$\beta=2\left(\frac{\partial x}{\partial\phi}\frac{\partial x}{\partial\psi}+\frac{\partial y}{\partial\phi}\frac{\partial y}{\partial\psi}\right) \tag{5}$$

$$\gamma=4\left(\left(\frac{\partial x}{\partial\phi}\right)^2+\left(\frac{\partial y}{\partial\phi}\right)^2\right) \tag{6}$$

We wish to generalize the method so that the different resolution levels in the Dynamic Mesh do not cause the finer meshing to spread into the coarser regions at resolution transitions. The disjoint nodes are slaved and do not need to be considered during relaxation.

The differences in the nodal length spacings are taken into account by giving each node length values, for example $Cx_{\phi+1,\psi+1}$ and $Cy_{\phi+1,\psi+1}$, denoting if it is coarse or finely spaced from the centre node in that direction (refer to Figure 1). Taylor series expansions involving the length values are then used to discretize the derivatives. The resulting relaxation equation weights depend on the length values. The four nearest neighbour nodes only require one value, such as $C_{\phi,\psi+1}$, as there is only one direction of spacing from the centre node. The weights for the x-coordinate relaxation were calculated using the Cx's and the weights for the y-coordinate relaxation using the Cy's.

The mixed derivative for the x-coordinate is discretized using Taylor series expansions for the corner nodes, for example

$$x_{\phi+1,\psi+1}=x_{\phi,\psi}+Cx_{\phi+1,\psi+1}l\left(\frac{\partial x}{\partial\phi}\right)+Cx_{\phi+1,\psi+1}h\left(\frac{\partial x}{\partial\psi}\right)\dots \tag{7}$$

The mixed derivative discretization is

$$\begin{aligned}\frac{\partial^2 x}{\partial\phi\psi} = &-\frac{Cx_{\phi+1,\psi-1}Cx_{\phi-1,\psi+1}-Cx_{\phi+1,\psi+1}Cx_{\phi-1,\psi-1}}{2lhCx_{\phi+1,\psi+1}Cx_{\phi+1,\psi-1}Cx_{\phi-1,\psi+1}Cx_{\phi-1,\psi-1}}x_{\phi,\psi}\\ &+\frac{x_{\phi+1,\psi+1}}{2lh(Cx_{\phi-1,\psi-1}Cx_{\phi+1,\psi+1}+Cx^2_{\phi+1,\psi+1})}\\ &-\frac{x_{\phi-1,\psi+1}}{2lh(Cx_{\phi-1,\psi+1}Cx_{\phi+1,\psi-1}+Cx^2_{\phi-1,\psi+1})}\\ &-\frac{x_{\phi+1,\psi-1}}{2lh(Cx_{\phi-1,\psi+1}Cx_{\phi+1,\psi-1}+Cx^2_{\phi+1,\psi-1})}\\ &+\frac{x_{\phi-1,\psi-1}}{2lh(Cx_{\phi-1,\psi-1}Cx_{\phi+1,\psi+1}+Cx^2_{\phi-1,\psi-1})}\end{aligned} \tag{8}$$

where the l's and h's will cancel out in the inverse equation.

The other derivatives and the α's, β's and γ's are discretized using similar principles. Substituting into the inverse equation results in the following formula for the new x nodal coordinate:

$$\begin{aligned}x_{\phi,\psi} = &\frac{\alpha_{\phi,\psi}\left(\dfrac{x_{\phi-1,\psi}}{C_{\phi-1,\psi}}+\dfrac{x_{\phi+1,\psi}}{C_{\phi+1,\psi}}\right)}{D(C_{\phi,\psi+1}+C_{\phi,\psi-1})^2(C_{\phi-1,\psi}+C_{\phi+1,\psi})}\\ &+\frac{\gamma_{\phi,\psi}\left(\dfrac{x_{\phi,\psi-1}}{C_{\phi,\psi-1}}+\dfrac{x_{\phi,\psi+1}}{C_{\phi,\psi+1}}\right)}{D(C_{\phi+1,\psi}+C_{\phi-1,\psi})^2(C_{\phi,\psi-1}+C_{\phi,\psi+1})}\\ &+\frac{\beta_{\phi,\psi}\left(\dfrac{\left(\dfrac{x_{\phi-1,\psi+1}}{Cx_{\phi-1,\psi+1}}+\dfrac{x_{\phi+1,\psi-1}}{Cx_{\phi+1,\psi-1}}\right)}{(Cx_{\phi-1,\psi+1}+Cx_{\phi+1,\psi-1})}-\dfrac{\left(\dfrac{x_{\phi+1,\psi+1}}{Cx_{\phi+1,\psi+1}}+\dfrac{x_{\phi-1,\psi-1}}{Cx_{\phi-1,\psi-1}}\right)}{(Cx_{\phi+1,\psi+1}+Cx_{\phi-1,\psi-1})}\right)}{D(C_{\phi+1,\psi}+C_{\phi-1,\psi})(C_{\phi,\psi+1}+C_{\phi,\psi-1})}\end{aligned} \tag{9}$$

where D is given by

$$\begin{aligned}D = &\frac{\alpha_{\phi,\psi}}{(C_{\phi,\psi+1}+C_{\phi,\psi-1})^2(C_{\phi-1,\psi}C_{\phi+1,\psi})}\\ &+\frac{\gamma_{\phi,\psi}}{(C_{\phi+1,\psi}+C_{\phi-1,\psi})^2(C_{\phi,\psi-1}C_{\phi,\psi+1})}\\ &+\frac{\beta_{\phi,\psi}(Cx_{\phi+1,\psi+1}Cx_{\phi-1,\psi-1}-Cx_{\phi+1,\psi-1}Cx_{\phi-1,\psi+1})}{\Pi(C_{\phi+1,\psi}+C_{\phi-1,\psi})(C_{\phi,\psi+1}+C_{\phi,\psi-1})}\end{aligned} \tag{10}$$

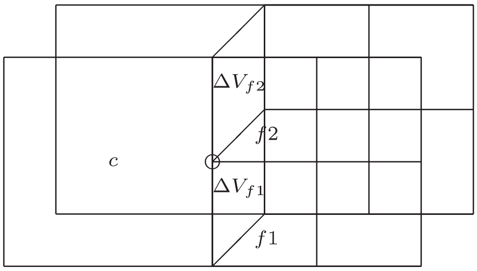

Figure 2. Overlap volumes for advection.

Table I. Errors for fine, anisotropic and coarse radial Sod calculations $t = 0.25$.

Calculation	$\|e\|_1$	$\|e\|_2$
Fine	0.0044	0.0105
Anisotropic	0.0046	0.0107
Coarse	0.0072	0.0139

with

$$\Pi = Cx_{\phi+1,\psi+1} Cx_{\phi+1,\psi-1} Cx_{\phi-1,\psi+1} Cx_{\phi-1,\psi-1} \tag{11}$$

We express this formula in terms of the $\alpha_{\phi,\psi}$, $\beta_{\phi,\psi}$ and $\gamma_{\phi,\psi}$ used in the original method. The expression for the y-coordinate has a similar form. The method automatically reduces to the isotropic case if the Cx's are equal to the Cy's and reduces to the original Winslow–Crowley relaxation equations if the nodal spacings are also all the same.

The remapping or advection method [1] is generalized for the Dynamic Mesh by considering all neighbours that fluxes are passed to, summing all fine fluxes that are passed to a coarse element, and constructing fine fluxes as an overlap volume weighted ratio of the coarse flux on that side [8]. Figure 2 illustrates the overlap volumes at a resolution transition. To remap the nodal velocities a dual mesh is constructed, since no nodal mass is associated with the disjoint nodes they do not have dual cells surrounding them and the dual mesh line passes straight through each disjoint node [8].

3. RESULTS

The anisotropic refinement ALE method was tested on a radial Sod problem [9] with an initially 50 × 50 mesh that was then refined. The refinement radius was 0.04 and the derefinement threshold was 0.025. Refined regions occurred around the rarefaction fan, contact and shock, with derefinement in between these features. The majority of the refinement was anisotropic, with isotropic refinement only within 15–20° of the diagonal. The adaptive mesh and density contours are shown in Figure 3. The errors for the adaptive calculation, given in Table I, are comparable with the uniformly fine calculation errors and are far better than the coarse calculation errors. The anisotropic calculation only requires 32% of the fine calculation's number of elements and runs 7.8 times faster than the uniformly fine calculation.

DOI: 10.1002/fld

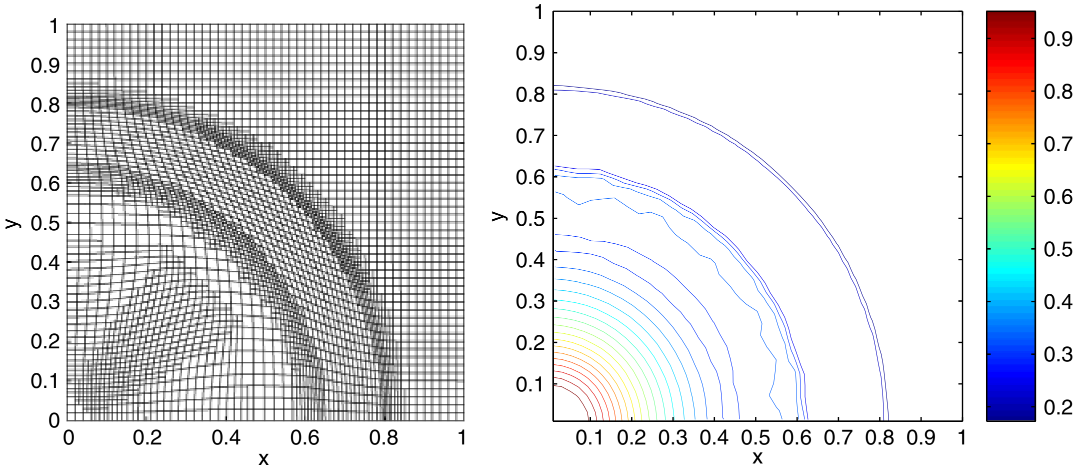

Figure 3. Radial Sod problem anisotropic mesh and density contours at $t = 0.25$.

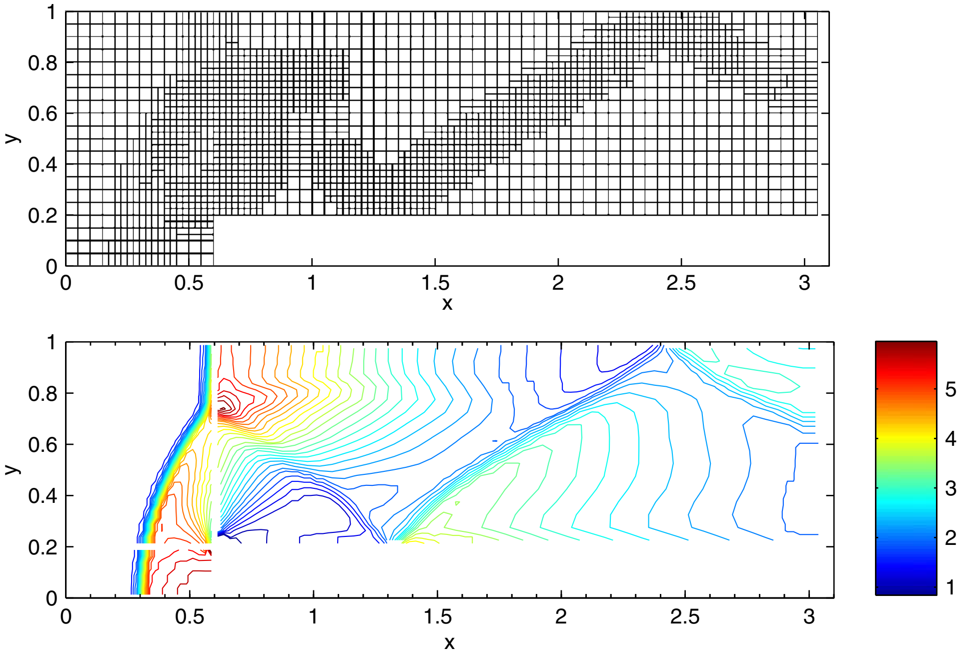

Figure 4. Mach 3.0 step problem anisotropic mesh and density contours at $t = 4.0$.

The method has also been tested on the Woodward and Colella Mach 3 step problem [10], which contains many sensitive features of interest. In this problem the solution is remapped back to a fixed Eulerian mesh every time step, rather than using mesh relaxation. The method has refined the shocks, Mach stem and contact, with anisotropic refinement occurring where the features align with the mesh as shown in Figure 4. The anisotropic density contours, see Figure 4, are very similar to those obtained from the uniformly fine calculation. The Mach stem is situated above the step and its length is comparable with that shown in Woodward and Colella [10]. The anisotropic calculation only requires 45% of the number of elements and runs 4 times faster than the uniformly fine calculation.

ACKNOWLEDGEMENTS

We wish to thank Chris Powell for his help with the isotropic adaptive mesh code.

REFERENCES

1. Barlow A. An adaptive multi-material Arbitrary Lagrange Eulerian algorithm for computational shock hydrodynamics. *Ph.D. Thesis*, Swansea, 2002.
2. Peery J, Carroll D. Multi-material ALE methods in unstructured grids. *Computer Methods in Applied Mechanics and Engineering* 2000; **187**:591–619.
3. Winslow AM. Numerical solution of the quasilinear poisson equation in a non-uniform triangular mesh. *Journal of Computational Physics* 1966; **1**:149–172.
4. Aftosmis M. Upwind method for simulation of viscous flow on adaptively refined meshes. *AIAA Journal* 1994; **32**(2):268–277.
5. Berger MJ, Colella P. Local adaptive mesh refinement for shock hydrodynamics. *Journal of Computational Physics* 1989; **82**:64–84.
6. Anderson RW, Elliott NS *et al.* An Arbitrary Lagrangian–Eulerian method with adaptive mesh refinement for the solution of the Euler equations. *Journal of Computational Physics* 2004; **199**:598–617.
7. Plewa T, Linde T, Weirs VG. *Adaptive Mesh Refinement—Theory and Applications*. Springer: Berlin, 2005.
8. Morrell JM, Sweby PK, Barlow A. A cell by cell anisotropic adaptive mesh ALE scheme for the numerical solution of the Euler equations. *Journal of Computational Physics* 2007; **226**(1):1152–1180.
9. Toro EF, *Riemann Solvers and Numerical Methods for Fluid Dynamics* (2nd edn). Springer: Berlin, 1999.
10. Woodward P, Colella P. The numerical simulation of two-dimensional fluid flow with strong shocks. *Journal of Computational Physics* 1984; **54**:115–173.

DOI: 10.1002/fld